

# Deformed strangelets at finite temperature

Munshi Golam Mustafa\*

*Variable Energy Cyclotron center, 1/AF Bidhan Nagar, Calcutta 700 064*

A. Ansari †

*Institute of Physics, Bhubaneswar 751005, India.*

(August 11, 2018)

## Abstract

Considering the confinement of massless  $u$  and  $d$  quarks and massive  $s$  quarks in an axially symmetric quadrupole shaped deformable bag, the stability properties of color-singlet strangelets at finite temperatures are studied for the baryon number  $A \leq 100$ . It is found that, in general, at each  $A$  the energy of the strangelet is the lowest for the spherical shape. However, it is interesting to find shell structures for the deformed shapes at some new  $A$  values, not found for the spherical shape. This should be of relevance for the experimental search of strangelets. The color projected (singlet) calculation shows that even for the deformed shapes the shell structures vanish only for the temperature,  $T \gtrsim 30$  MeV. On the other hand, from a somewhat crude estimate we also find that at a fixed entropy per baryon (instead of a fixed temperature) of the order of unity or higher these shell structures disappear. PACS numbers: 12.38.Aw, 12.38.Mh, 12.40.Aa, 24.85.+p

Typeset using REVTeX

---

\*Electronic Address: mustafa@veccal.ernet.in

†Electronic Address: ansari@iop.ren.nic.in

## I. INTRODUCTION

The stability properties of very small strangelets (baryon number  $A \leq 100$ ) were studied recently by Gilson and Jaffe [1] and others [2] in the independent particle spherical shell model picture where massless  $u$  and  $d$  quarks, and massless or massive  $s$  quarks are considered to be confined in a spherical bag with a bag pressure constant,  $B$ . In view of the hot environment of ultrarelativistic heavy-ion collisions where strangelets may be formed, we have recently [3,4] extended the work of Ref. [1] to finite temperatures using the method of statistical mechanics. At a finite temperature ( $T > 0$ ), for a given baryon number,  $A$ , a partition function is constructed using the eigen-energies of the non-interacting ( $3A$ ) quarks confined in the bag. Then the free energy of the system is minimized with respect to the radius of the bag leading to the minimum energy of the system at that  $T$ . For  $T = 0$  we actually consider  $T = 1$  MeV and find [3,4] that the results are similar to those in Ref. [1]. At high temperatures ( $T \gtrsim 10$  MeV) we construct explicitly, following projection techniques [4,5], a color-singlet partition function. At a given  $T$  and  $A$  the color projection (CP) leads to lowering of the energy as compared to the unprojected case and when there are shell closures, the shell pockets become deeper. After CP some of the shell closure positions also get shifted to other  $A$  values. Using  $B^{1/4} = 145$  MeV with massless  $u$  and  $d$  quarks, and massive  $s$  quarks ( $m_s = 150$  MeV) we found in Ref. [4] that in the bulk limit,  $A \geq 100$ , CP has little effect and results are similar to those of the liquid drop model calculations of Jensen and Madsen [6]. It is also found in Ref. [4] that for  $T \gtrsim 30$  MeV shell structures melt away.

Now, coming back to the main topic of shape deformation, we know that many nuclei are deformed in the ground state, and this happens simply due to the effect of shell structures (quantal effect). Therefore, it should be worthwhile to investigate the stability properties of strangelets allowing for the deformation degrees of freedom at  $T = 0$  as well as at  $T > 0$ . Using the same formalism as earlier [4] these calculations can be carried out if the quark eigen-modes in the deformed bag are known. Actually following the formalism developed by

Viollier, Chin and Kerman [7] to compute the single-particle energies of quarks and gluons in a spheroidal bag, we have already made a study [8] of the thermodynamics of a deformed bag with  $A = 1$  considering two flavors of quarks  $u$  and  $d$ , and gluons. In the present work the considered values of temperatures are very low ( $T = 1$  and  $20$  MeV) and so like in Refs. [3,4] here too we have not included gluons in our calculations.

## II. FORMALISM

The formalism is essentially that of Ref. [4] except that now the input single-particle energies depend on the quadrupole deformation parameter which is an additional degree of freedom. The computations being quite time consuming we have considered only two values of the temperature  $T = 1$  and  $20$  MeV.

Introducing a deformation parameter,  $D$ , the surface of a spheroidal bag, in the body-fixed frame, is given by

$$Dx^2 + Dy^2 + D^{-2}z^2 = R_0^2, \quad (1)$$

where  $R_0$  is the radius of a sphere with the same equivalent volume. From Eq. (1) it is clear that the semi-major and semi-minor axes of the spheroid are  $DR_0$  and  $R_0D^{-1/2}$ , respectively, with a volume clearly independent of  $D$ . For  $D = 1$  the shape is obviously spherical. A radial coordinate at the surface of the spheroid is given by

$$R(\theta) = R_0 \left[ a(D) + \sqrt{\frac{2}{3}} b(D) P_2(\cos \theta) \right]^{-1/2}, \quad (2)$$

with

$$a(D) = \frac{1}{3} (2D + D^{-2}), \quad (3)$$

and

$$b(D) = -\sqrt{\frac{2}{3}} (D - D^{-2}), \quad (4)$$

where  $P_2(\cos\theta)$  is the standard Legendre polynomial of order 2. The details of the calculations of the eigenmodes for the quarks confined in the cavity described by Eq. (1) or Eq. (2) are as given in Refs. [7,8]. The problem is reduced to the diagonalization of a real non-symmetric matrix for a fixed parity. The eigenvalues are functions of  $R_0$  and  $D$  where  $R_0$  enters actually as  $\hbar c/R_0$  with  $\hbar c = 197.32$  MeV fm.

The color-singlet partition function is given by [4,5]

$$\mathcal{Z}_C(T, R_0, D) = \int_{\text{SU}(3)} d\mu(g) \text{Tr} \left( \hat{U}(g) e^{-\hat{H}/T} \right), \quad (5)$$

where  $\hat{H}$  denotes the Hamiltonian of the system and

$$\int_{\text{SU}(N_C)} d\mu(g) = \frac{1}{N_C!} \left( \prod_{i=1}^{N_C-1} \int_{-\pi}^{\pi} \frac{d\theta_i}{2\pi} \right) \left[ \prod_{j<k}^{N_C} \left( 2 \sin \frac{\theta_j - \theta_k}{2} \right)^2 \right], \quad (6)$$

with  $N_C = 3$  for SU(3) color group. The chemical potential ( $\mu_q = -\mu_{\bar{q}}$ ) dependent partition function can be written as [4]

$$\mathcal{Z}_C(T, R_0, D, \mu_q) = \int_{\text{SU}(3)} d\mu(g) e^{\Theta}, \quad (7)$$

with

$$\begin{aligned} \Theta = & \frac{1}{2} \sum_{\alpha} \ln \left( 1 + f_{\alpha}^{q^2} + 2f_{\alpha}^q \cos \theta_1 \right) + \frac{1}{2} \sum_{\alpha} \ln \left( 1 + f_{\alpha}^{q^2} + 2f_{\alpha}^q \cos \theta_2 \right) \\ & + \frac{1}{2} \sum_{\alpha} \ln \left[ 1 + f_{\alpha}^{q^2} + 2f_{\alpha}^q \cos(\theta_1 + \theta_2) \right] + \frac{1}{2} \sum_{\alpha} \ln \left( 1 + f_{\alpha}^{\bar{q}^2} + 2f_{\alpha}^{\bar{q}} \cos \theta_1 \right) \\ & + \frac{1}{2} \sum_{\alpha} \ln \left( 1 + f_{\alpha}^{\bar{q}^2} + 2f_{\alpha}^{\bar{q}} \cos \theta_2 \right) + \frac{1}{2} \sum_{\alpha} \ln \left[ 1 + f_{\alpha}^{\bar{q}^2} + 2f_{\alpha}^{\bar{q}} \cos(\theta_1 + \theta_2) \right], \end{aligned} \quad (8)$$

where  $f_{\alpha}^q = e^{-\beta(\epsilon_{\alpha}^q - \mu_q)}$  and  $f_{\alpha}^{\bar{q}} = e^{-\beta(\epsilon_{\alpha}^{\bar{q}} + \mu_q)}$ .

In Eq. (8)  $\beta = 1/T$  is the usual inverse temperature with  $T$  taken in the units of energy (here MeV) and  $\epsilon_{\alpha}^q$  represents the  $R_0$  and  $D$  dependent quark(antiquark) single-particle energies with  $\alpha$  denoting the single-particle state labels (spherical or deformed). The upper limit of the summation  $\alpha$  depends upon the value of  $A$  and  $T$ , such that further inclusion of states in the summation does not affect the results. In this sum the summation over quark flavors  $u$ ,  $d$ , and  $s$  is also understood. The color unprojected (CUP) partition function is simply given by

$$\mathcal{Z}_U(\beta, R_0, D, \mu_q) = e^\Theta , \quad (9)$$

where now

$$\Theta = \sum_{\alpha} \left[ \ln \{1 + e^{-\beta(\epsilon_q^{\alpha} - \mu_q)}\} + \ln \{1 + e^{-\beta(\epsilon_q^{\alpha} + \mu_q)}\} \right] . \quad (10)$$

As usual the particle number for a given flavour is calculated from

$$N_q = T \frac{\partial}{\partial \mu_q} (\ln \mathcal{Z}) , \quad (11)$$

where  $\mathcal{Z}$  is given by Eq. (7) or Eq. (9), as the case may be. The baryon number  $A$  is fixed by adjusting the value of the quark chemical potential such that the excess number of  $q$  over  $\bar{q}$  is  $3A$ :

$$(N_u - N_{\bar{u}}) + (N_d - N_{\bar{d}}) + (N_s - N_{\bar{s}}) = 3A . \quad (12)$$

The free energy of the system is given by

$$F(T, R_0, D) = -T \ln \mathcal{Z} + 3\mu_q A + BV . \quad (13)$$

With the above definition of free energy, the condition of stability is given by

$$P = - \left( \frac{\partial}{\partial V} F(T, R_0, D) \right)_{T,A} = 0 . \quad (14)$$

This way at a given  $T$  and  $D$ , the bag radius parameter  $R_0$  is determined. We may call  $R_0$  a radius parameter in the sense that for a deformed bag it is not actually the radius. In practice we minimize the free energy with respect to  $R_0$ , keeping at each step the number Eq. (12) satisfied. Then the energy of a strangelet is computed from

$$E(T, R_0, D) = T^2 \frac{\partial}{\partial T} (\ln \mathcal{Z}) + 3\mu_q A + BV , \quad (15)$$

where  $BV$  is the bag volume energy.

### III. RESULTS AND DISCUSSIONS

After solving Eqs. (12) and (14) selfconsistently for a given  $A$ ,  $T$  and  $D$  the energy (mass) of a strangelet is computed according to Eq. (15). As in our earlier works [3,4], here, too, we have taken  $B^{1/4} = 145$  MeV, massless  $u$  and  $d$ , and massive  $s$  quarks, ( $m_s = 150$  MeV). The variation of the energy per baryon ( $E/A$ ) as a function of  $A$  is plotted in Fig. 1a for  $T = 1$  MeV (practically the ground state) for spherical and prolate shapes with  $D = 1.0, 1.2, 1.4, 1.6, 1.8,$  and  $2.0$ . A similar plot is shown in Fig. 1b for  $D = 1.0, 0.8$  and  $0.6$ ; for  $D < 1$  the shape is oblate. From Eq. (1) it is clear that the ratio of the semi-major axis ( $a$ ) to semi-minor axis ( $b$ ) of the spheroid is  $D^{3/2}$  from which (just to give an idea of the extent of deformation) it also follows that approximately  $a = 0.5b, 2b$  and  $3b$  for  $D = 0.6, 1.6$  and  $2.0$ , respectively. These  $a$  and  $b$  should not be confused with those defined through Eqs. (3) and (4). From Figs. 1a and 1b it is clear that, in general, the shell structure is persisting even if the shape of the bag (strangelet) is deformed, though energetically at every  $A$  the spherical shape leads to the lowest energy configuration. The shell positions at various baryon numbers ( $A_{sh}$ ) are shown more explicitly in Table I. One new thing we find is that with the increase of deformation (prolate as well as oblate) the shell structure at  $A = 18$  is vanishing and, on the contrary, the shell structure at  $A = 14$  is becoming more pronounced.

In Figs. 2a and 2b we display the variation of the strangeness (actual value is negative) as a function of  $A$  for the prolate and oblate shapes, respectively at  $T = 1$  MeV. In each figure the  $D = 1$  (spherical) case is presented for the sake of comparison. In the spherical case we have steplike structure with well-known loading - unloading characteristics near  $A = 20$  [1]. With the increase of deformation the curves are becoming smoother, though still some oscillation persists, as expected, at  $T = 0$ .

In Fig. 3 we again show the plot of  $E/A$  vs  $A$  for various prolate shapes, like in Fig. 1a, but now at  $T = 20$  MeV when the color projected (singlet) and color unprojected (CUP) curves become distinguishable. For the CUP case there is hardly any shell structure except near  $A = 6$  for  $D = 1.0$ . As can be seen from Table II, this is actually at  $A = 5$  with a

small pocket of about 1.0 MeV with the number of  $s$ -quark,  $n_s = 2$  (see strangeness vs  $A$  plot in Fig. 4). On the other hand, for CP case and  $D=1.0-1.6$ , the shell structure appears only at  $A = 4$  with  $n_s = 0$ . For  $A > 4$  the strangeness number becomes non-zero, so much so that even at  $A = 5$  and  $D = 1$ ,  $n_s=2.3$ . As Fig. 4 shows, for  $A > 10$  or so, the  $S$  vs  $A$  curve becomes almost a straight line ( $S/A \sim 0.5-0.6$ ) with the strangeness content slightly increasing with the increase of deformation. One striking thing in Fig. 3 for the CP case is the development of a shell structure at  $A = 15$  with the increase of deformation. As can be seen from Table II, this shell pocket at  $A = 15$  is 0.6 MeV with number of  $s$ -quark,  $n_s \sim 7$ .

From the discussions so far, it is clear that the color-singlet constraint leads to more pronounced shell structures. For  $T = 20$  MeV and  $D=1.0, 1.4$  and  $2.0$  we demonstrate it in Fig. 5 through a plot of a type of color-correlation energy  $\Delta E = E^{\text{CUP}}/A - E^{\text{CP}}/A$  vs  $A$ . It clearly shows the magnified effect of color projection near the shell closures. In this figure the first high peak is exactly at  $A = 4$  whereas the second one is at  $A = 14$  with  $A = 13$  and  $15$  lying quite nearby. It is interesting to notice that, though for  $D = 1.0$  there is a clear-cut shell pocket at  $A = 14$  in the  $E/A$  vs  $A$  plot, the effect of the gain in energy due to color projection is getting highly focussed in the present plot. On the whole for  $A > 6$  the effect of color projection seems somewhat stronger for  $D > 1$  but again for  $D > 1.2$  and  $A > 20$  it shows a kind of saturation as far as the large values of  $D$  are concerned.

Finally we want to discuss the effect of deformation vis-a-vis mass of the  $s$ -quark. Like in our previous work [4], here, too, we have considered two values,  $m_s = 0$  and  $150$  MeV. The  $E/A$  vs  $A$  plot at  $T = 1$  MeV is shown in Fig. 6 for  $m_s = 0$  (solid curve) and  $m_s = 150$  MeV (dashed) for  $D = 1.0$  (lower curve),  $1.4$  (middle) and  $2.0$  (upper). Again at each  $A$  the energy is the lowest for the spherical shape. The positions and the magnitudes of the shell structures are also enumerated in Table III for  $m_s = 0$  (see Table I for  $m_s = 150$  MeV). For  $m_s = 0$  a good (deep) shell structure at  $A = 6$  persists even with the increase of prolate deformation (oblate not considered) unlike in the case of massive  $s$ -quark. Also at  $A = 18$  a deeper shell structure develops with the increase of the prolate deformation in contrast to the opposite trend for  $m_s = 150$  MeV at the same baryon number, but rather

similar to that at  $A = 14$  when  $m_s = 150$  MeV.

For the  $m_s = 0$  case at  $T = 20$  MeV only the CP case is considered and the  $E/A$  vs  $A$  plot for both  $m_s = 0$  (solid) and 150 MeV (dashed) is displayed in Fig. 7 for  $D = 1.0$  (lower), 1.4 (middle) and 2.0 (upper). For  $m_s = 150$  MeV and  $D = 1.0$  and 1.4 the only shell structure seen is at  $A = 4$  with  $n_s = 0$ , whereas for  $D = 2.0$  a shell structure has developed at  $A = 15$  (see Table II). It is rather surprising to see that with  $m_s = 0$  the shell structure at  $A = 6$  is 27.11 MeV, 22.34 MeV and 16.31 MeV deep for  $D = 1.0, 1.4$  and 2.0, respectively which are even slightly deeper than that at  $T = 1$  MeV. Though this feature appears very interesting, it can not be given much importance as  $m_s = 0$  is unphysical. But it does highlight that the quantal features of the strangelets, particularly for  $A < 50$ , are quite sensitive to the mass of the  $s$ -quark.

Before presenting finally our conclusions in the next section we wish to make some comments, in view of the work of Ref. [6], on the shell structure features if the  $E/A$  vs  $A$  plot is made at a fixed entropy per baryon ( $s$ ). From our color projected numbers at  $D=1$  and  $T = 1, 10, 20, 30$  MeV we have computed  $s = (E/A - F/A)/T$  at these temperatures. Then a crude graphical interpolation analysis shows that for  $s \gtrsim 1.0$  there appear no shell structures. It seems somewhat surprising but a very interesting result in view of what we have discussed so far at fixed temperatures.

#### IV. CONCLUSIONS

We have investigated the stability properties of color-singlet strangelets at finite temperature within an axially symmetric quadrupole shape deformable MIT bag model. We find that at each baryon number  $A$  ( $\leq 100$ ) energetically a spherical shape is preferred at zero as well as at a finite temperatures. However, with the increase of deformation we find that the shell closures at some  $A$  for the spherical shape disappear and some new ones appear at different  $A$  values. This should have important implications in the experimental search of strangelets. The maximum deformed ( $D = 2.0$ ) prolate shape is considered such that the



ratio of the semi-major to semi-minor axis is about 3:1. On the considered oblate side ( $D = 0.6$ ) this ratio is 1:2. At a finite temperature,  $T = 20$  MeV in the CP calculation the shell closure occurs at  $A = 4$  for  $D = 1.0, 1.2$  and  $1.6$  which is actually a lump of  $u$  and  $d$  quarks only. We may add that this point was missed in our earlier work of Ref. [4]. However, at  $D = 2.0$  and  $T = 20$  MeV a shell structure is found at  $A = 15$  with  $n_s = 7$ .

Considering massless  $s$  quarks ( $m_s = 0$ ), we get, in general, results similar to as discussed above (see Table III). However, for this case one interesting result is found that is at  $T = 20$  MeV the shell structure at  $A = 6$ , for  $D = 1.0, 1.4$  and  $2.0$ , is even slightly more pronounced than that at  $T = 1$  MeV.

It appears that in an  $E/A$  vs  $A$  plot at a fixed entropy per baryon ( $s$ ) there are no shell structures even for low values of  $s \sim 1.0$  and  $A \leq 30$ . A detailed shell model calculation within the present approach for  $s \leq 1.0$  and  $A \leq 30$  should be interesting for a proper analysis of the shell structures.

## REFERENCES

- [1] E. P. Gilson, and R. L. Jaffe, Phys. Rev. Lett. **71**, 332 (1993).
- [2] E. Farhi and R. L. Jaffe, Phys. Rev. D **30**, 2379 (1984); M. S. Berger and R. L. Jaffe, Phys. Rev. C **35**, 213 (1987); C. Greiner, D. -H. Rischke, H. Stoecker, and P. Koch, Phys. Rev. D **38**, 2797 (1988); J. Madsen, Phys. Rev. D **50**, 3328 (1994); **47**, 5156 (1993); Phys. Rev. Lett. **70**, 391 (1993).
- [3] M. G. Mustafa, and A. Ansari, Phys. Rev. D **53**, 5136 (1996); *ibid.* **54**, 4694(E) (1996).
- [4] M. G. Mustafa, and A. Ansari, Phys. Rev. C **55**, 2005 (1997).
- [5] G. Auberson, L. Epele, G. Mahoux and F. R. A. Simao, J. Math. Phys. **27**,1658 (1986); M. I. Gorenstein, S. I. Lipskikh, V. K. Petrov, and G. M. Zinovjev, Z. Phys. C **18**, 13 (1983); Phys. Lett. **123B**, 437 (1983); H. -T. Elze, W. Greiner and J. Rafelski, *ibid.* **124B**, 515 (1983).
- [6] D. M. Jensen, and J. Madsen, Phys. Rev. C **53**, R4719 (1996).
- [7] R. D. Violler, S. A. Chin and A. K. Kerman, Nucl. Phys. **A407**, 269 (1983).
- [8] A. Ansari, and M. G. Mustafa, Nucl. Phys. **A539**, 752 (1992).

TABLES

TABLE I. Shell positions at various baryon numbers ( $A_{\text{sh}}$ ) and the value of the pocket depth ( $E_{\text{sh}}$ ) defined as  $E_{\text{sh}} = (E/A_B - E/A_{\text{sh}})$  where  $A_B > A_{\text{sh}}$  and  $E/A_B$  has got the highest value. These are shown for  $T = 1$  MeV at a few values of the deformation parameter  $D$ .

$D$	$A_{\text{sh}}$	$A_B$	$E_{\text{sh}}$ (MeV)
1.0	6	7	6.30
	14	15	0.17
	18	22	4.37
	36	40	2.17
	44	47	0.8
	70	82	2.36
1.6	6	7	0.70
	14	16	2.24
	18	19	4.37
	36	41	1.09
	70	83	0.94
2.0	14	16	5.00
	36	42	1.34
	72	78	0.40
0.6	14	16	3.40
	40	42	0.43
	76	82	0.45

TABLE II. Same as Table I for  $T = 20$  MeV. Now color unprojected (CUP) and color-singlet (CP) both the cases are shown.

$D$	$A_{\text{sh}}$	$A_B$	$E_{\text{sh}}$ (MeV)	Case
1.0	5	6	0.9	CUP
1.2	5	6	0.2	CUP
1.0	4	7	6.0	CP
1.2	4	6	4.7	CP
1.6	4	6	0.2	CP
2.0	15	17	0.6	CP

TABLE III. Same as Table I with  $m_s=0$  for CP at  $T = 20$  MeV.

$D$	$A_{\text{sh}}$	$A_B$	$E_{\text{sh}}$ (MeV)
1.0	6	9	26.43
	18	19	0.25
	24	28	3.75
	42	50	4.50
	54	59	1.0
	84	100	4.86
1.4	6	8	18.55
	18	20	0.98
	24	26	0.89
	42	51	3.59
	84	100	4.14
2.0	6	8	13.66
	18	21	4.11
	42	51	3.52
	84	100	2.65

★ At  $A = 18$  a shell has developed with the increase of deformation and has vanished at  $A = 24$  and 54.

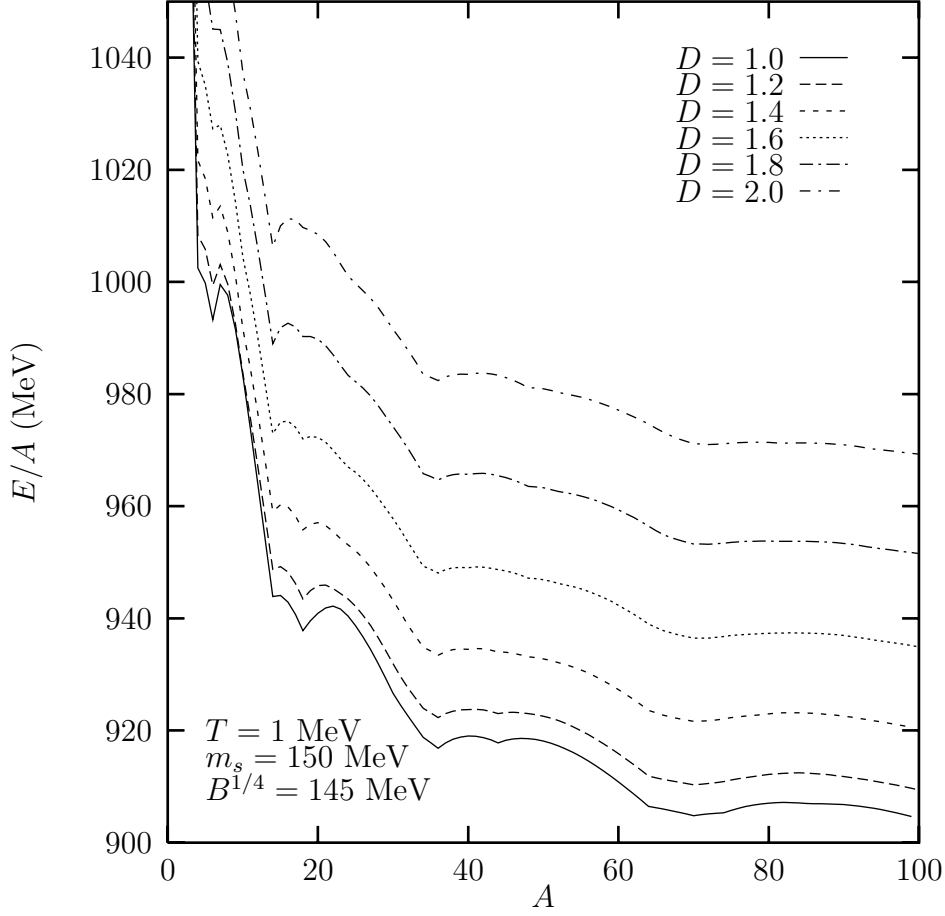


FIG. 1a. Baryon energy per particle ( $E/A$ ) as a function of  $A$  for various values of the deformation parameter ( $D=1.0, 1.2, 1.4, 1.6, 1.8$  and  $2.0$ ) with spherical and prolate shape at  $T=1 \text{ MeV}$ . The results are same for both colour projected (CP) and unprojected (CUP) cases at  $T=1 \text{ MeV}$ .

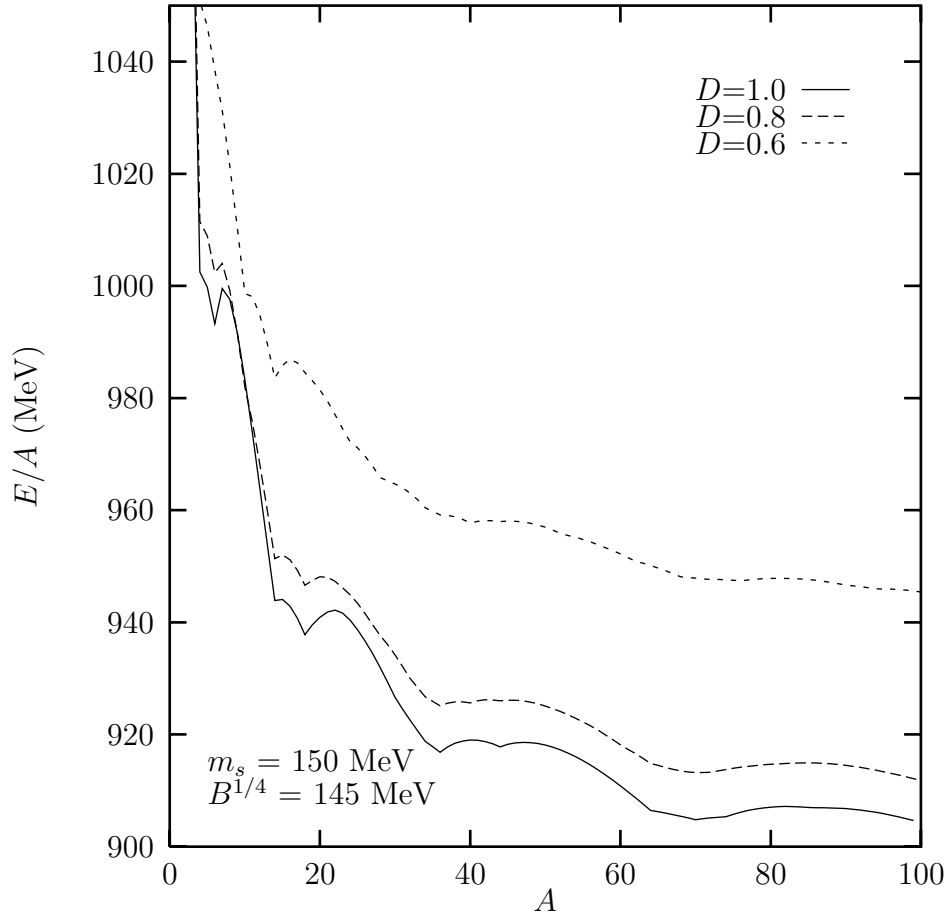


FIG. 1b. Same as FIG. 1a. with spherical and oblate shape for deformation parameter  $D = 1.0, 0.8$  and  $0.6$ .

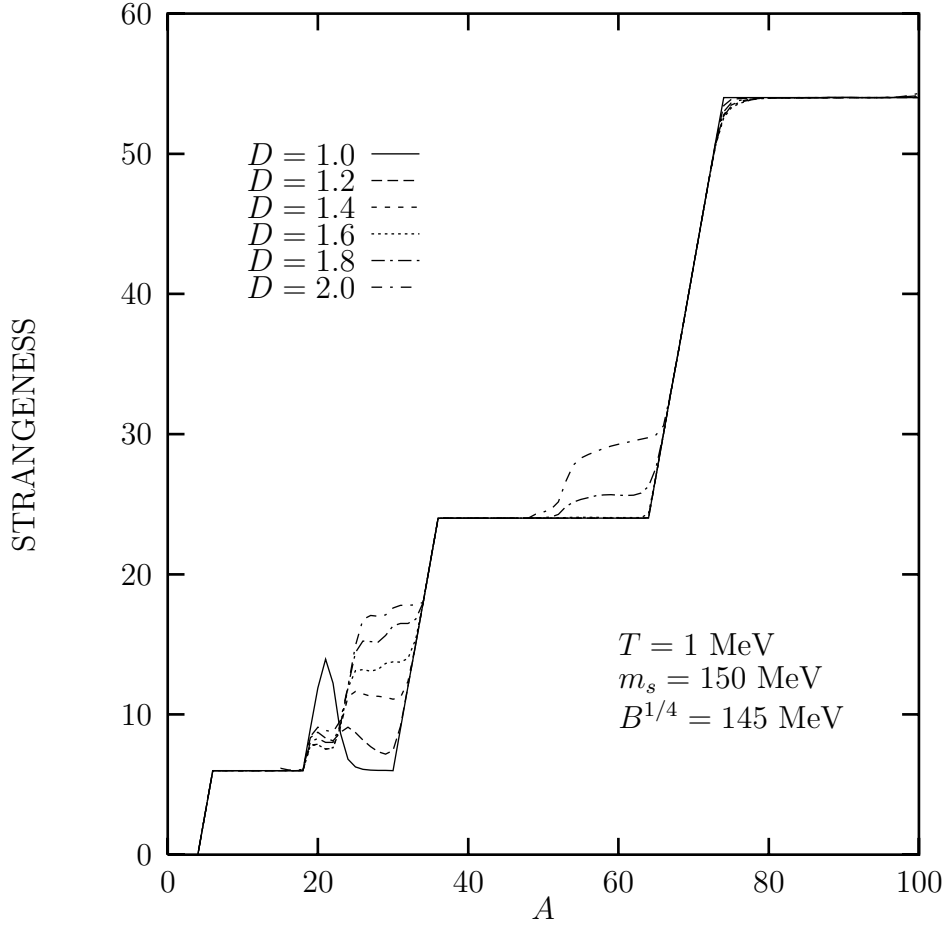


FIG. 2a. Strangeness as function of  $A$  for different values of  $D$  ( $= 1.0, 1.2, 1.4, 1.6, 1.8$  and  $2.0$ ) at  $T=1 \text{ MeV}$ .



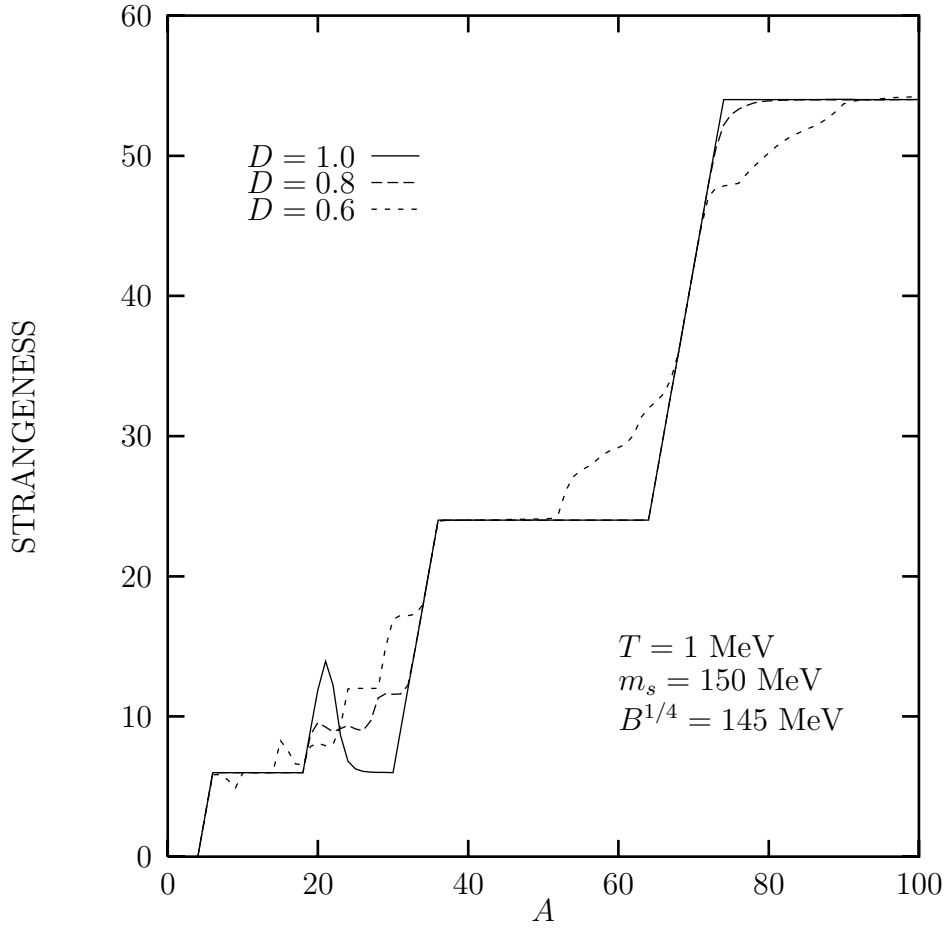


FIG. 2b. Same as FIG. 2a for  $D = 1.0, 0.8,$  and  $0.6$ .

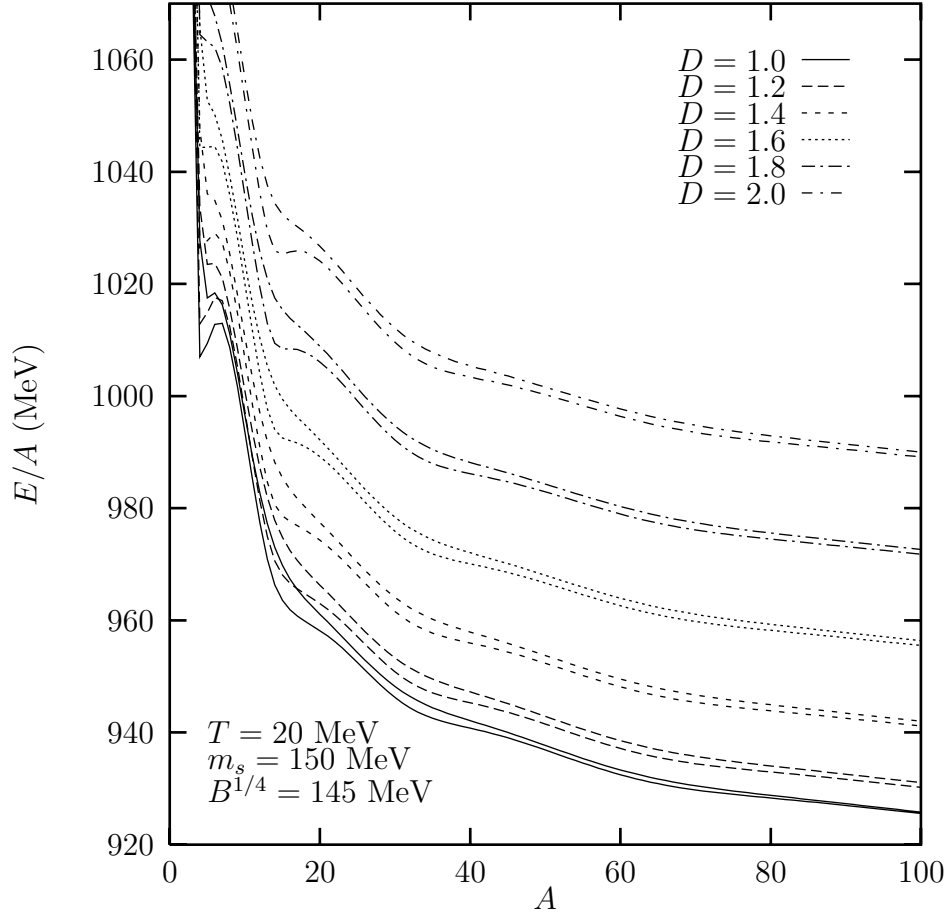


FIG. 3. Same as FIG. 1a with  $T = 20$  MeV and deformation values  $D = 1.0, \dots, 2.0$  for CP and CUP cases.

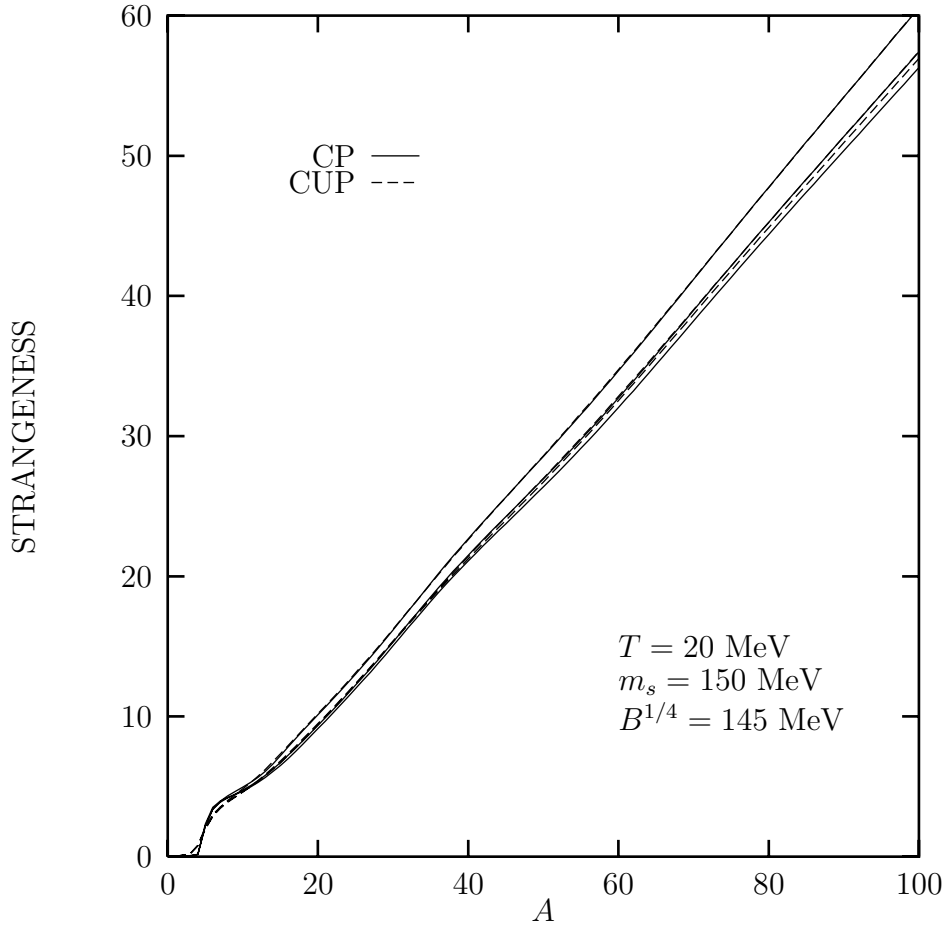


FIG. 4. Same as FIG. 2a with  $T=20$  MeV for the CP (continuous lines) as well as CUP (dashed lines) with  $D = 1.0, 1.4$  and  $2.0$  (Down to up).

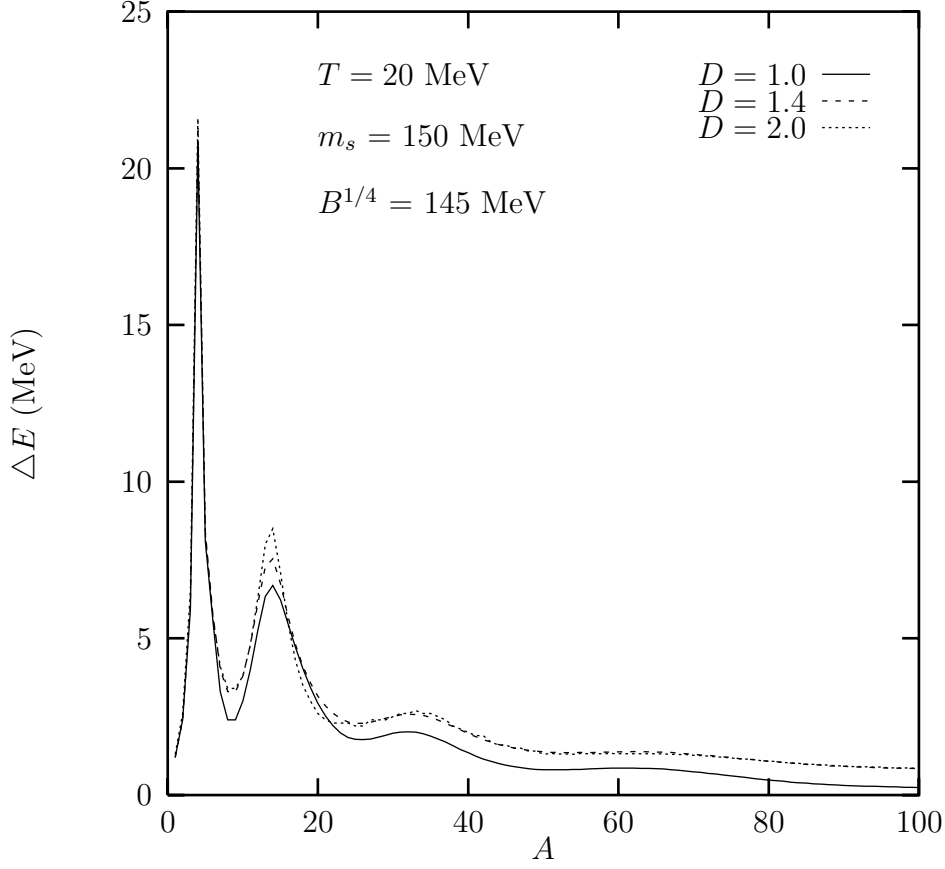


FIG. 5. The color-correlation energy defined as  $E^{\text{CUP}}/A - E^{\text{CP}}/A$  at  $T = 20 \text{ MeV}$  as function of  $A$  for  $D = 1.0, 1.4$  and  $2.0$ .

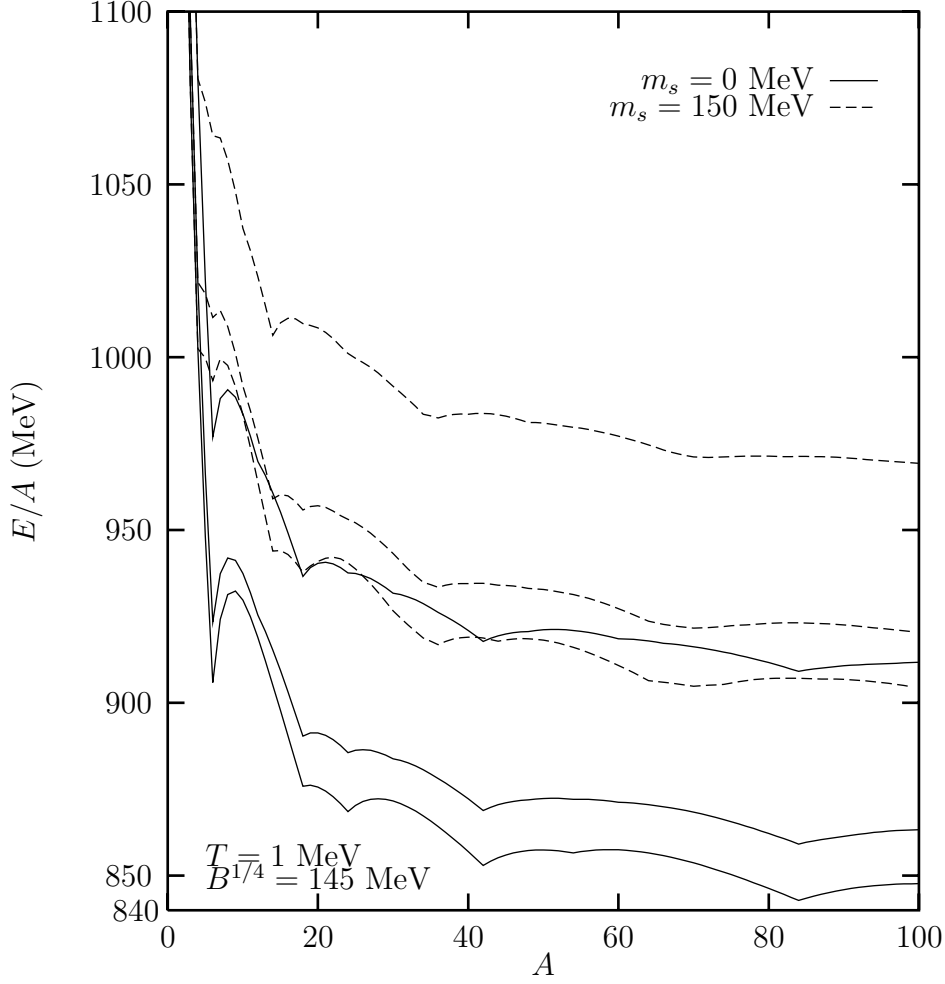


FIG. 6. Same as FIG. 1 for  $T = 1 \text{ MeV}$  with  $m_s = 0$  (continuous lines with  $D = 1$  (lower), 1.4 (middle) and 2.0 (upper)) and 150 MeV (dashed lines with  $D = 1$  (lower), 1.4 (middle) and 2.0 (upper)) in the CP scheme.

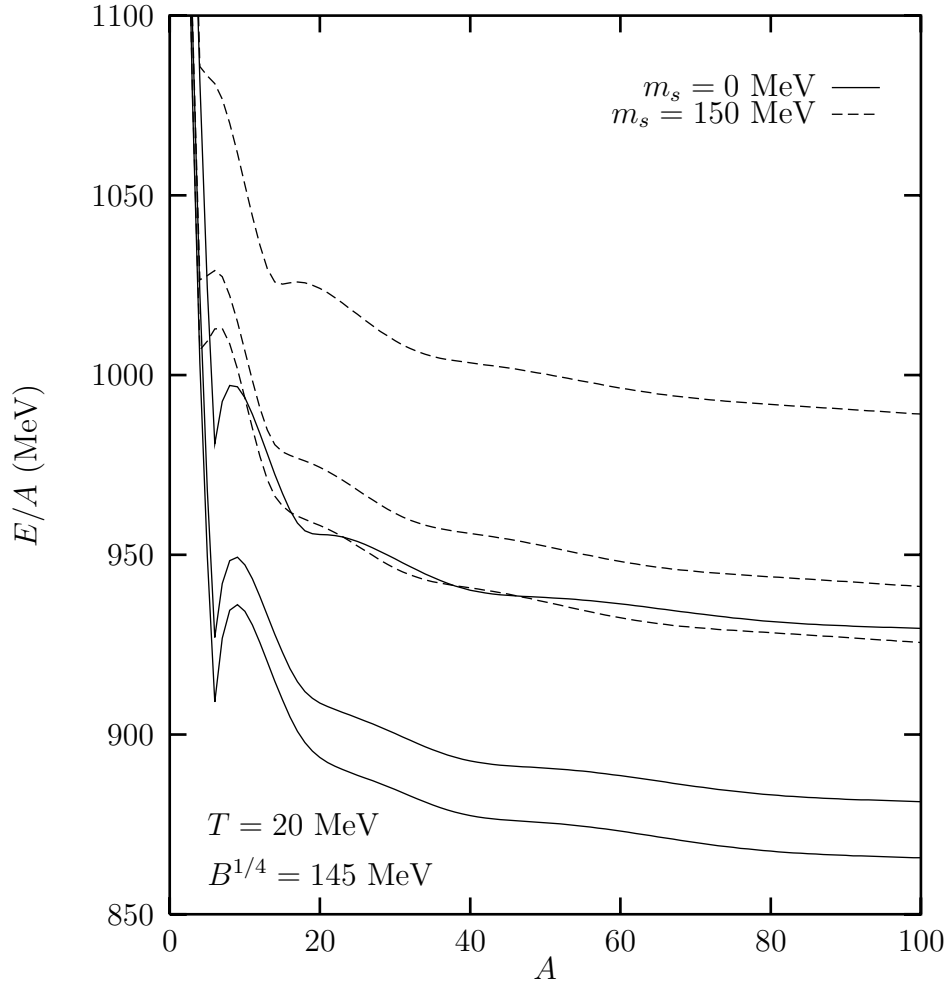


FIG. 7. Same as FIG. 6 with  $T = 20$  MeV.